Microsc. Microanal. Page 1 of 9
doi:10.1017/S1431927613001463

Microscopy AND Microanalysis



# Microstructural Characterization of Concrete Prepared with Recycled Aggregates

Mafalda Guedes,[1,2,*] Luís Evangelista,[3,4] Jorge de Brito,[4,5] and Alberto C. Ferro[2,6]

[1]*Department of Mechanical Engineering, Escola Superior de Tecnologia de Setúbal, Instituto Politécnico de Setúbal, 2910-761 Setúbal, Portugal*
[2]*ICEMS, Instituto Superior Técnico, Av. Rovisco Pais, 1049-001 Lisboa, Portugal*
[3]*Department of Civil Engineering, Instituto Superior de Engenharia de Lisboa, R. Conselheiro Emídio Navarro, 1, 1959-001 Lisboa, Portugal*
[4]*ICIST, Instituto Superior Técnico, Av. Rovisco Pais, 1049-001 Lisboa, Portugal*
[5]*Department of Civil Engineering, Architecture and Georesources, Instituto Superior Técnico, Universidade Técnica de Lisboa, Av. Rovisco Pais, 1049-001 Lisboa, Portugal*
[6]*Department of Mechanical Engineering, Instituto Superior Técnico, Universidade Técnica de Lisboa, Av. Rovisco Pais, 1049-001 Lisboa, Portugal*

**Abstract:** Several authors have reported the workability, mechanical properties, and durability of concrete produced with construction waste replacing the natural aggregate. However, a systematic microstructural characterization of recycled aggregate concrete has not been reported. This work studies the use of fine recycled aggregate to replace fine natural aggregate in the production of concrete and reports the resulting microstructures. The used raw materials were natural aggregate, recycled aggregate obtained from a standard concrete, and Portland cement. The substitution extent was 0, 10, 50, and 100 vol%; hydration was stopped at 9, 24, and 96 h and 28 days. Microscopy was focused on the cement/aggregate interfacial transition zone, enlightening the effect of incorporating recycled aggregate on the formation and morphology of the different concrete hydration products. The results show that concretes with recycled aggregates exhibit typical microstructural features of the transition zone in normal strength concrete. Although overall porosity increases with increasing replacement, the interfacial bond is apparently stronger when recycled aggregates are used. An addition of 10 vol% results in a decrease in porosity at the interface with a corresponding increase of the material hardness. This provides an opportunity for development of increased strength Portland cement concretes using controlled amounts of concrete waste.

**Key words:** concrete, construction and demolition waste, recycled fine aggregates, porosity, ITZ, microscopy

## Introduction

Construction throughout the world depends on concrete as a versatile, cheap, and efficient material. Concern regarding conservation of natural resources, shortage of waste land, the increasingly large volume of residues, and the high cost associated with treatment before disposal are driving growing interest in the recycling of construction and demolition waste (CDW). An interesting, yet challenging, application for recycled CDW is the replacement of natural aggregates (both fine and coarse) by recycled concrete aggregates (RCA) in the production of structural concrete. As aggregates in concrete comprise 60–75% of the total material volume (Cachim, 2009), any reduction in natural aggregate consumption is bound to have significant economic and environmental impact.

In the past few years, several authors have examined the viability of that substitution (e.g., Poon et al., 2004; Gomes & de Brito, 2009; Juan et al., 2010; Yang et al., 2011), finding satisfactory results concerning concrete workability, mechanical properties, and durability up to a limiting percentage of RCA substitution, which depends on the aggregate characteristics. This provides a window of opportunity for the use of increasingly large volumes of residues resulting from the construction and demolition sectors in the production of concrete.

Concrete is a composite mixture formed from cement, aggregates, water, and eventually admixtures or partial cement replacement materials. Setting and hardening of concrete occurs by a hydration reaction between the oxides in the cement and water, rendering a complex microstructure, which determines the properties of the hardened material. The main compounds in cement are $3CaO \cdot SiO_2$ (labeled $C_3S$ in cement chemistry shorthand notation), $2CaO \cdot SiO_2$ ($C_2S$), and $3CaO \cdot Al_2O_3$ ($C_3A$), and the solid solution with average composition $4CaO \cdot Al_2O_3 \cdot Fe_2O_3$ ($C_4AF$) (Domone, 1998). Each cement grain consists of an intimate mixture of these components. On hydration, $C_3A$ (and also $C_4AF$) reacts with gypsum ($CaO \cdot SO_3 \cdot 2H_2O$) to sequentially form the hydrous calcium aluminum sulfate ettringite $[Ca_6Al_2(SO_4)_3(OH)_{12} \cdot 26H_2O]$ (during approximately the first 24 h) and monosulfate $[3CaO \cdot (Al,Fe)_2O_3 \cdot CaSO_4 \cdot nH_2O]$ (afterwards). Once these initial reactions are complete, hydration reactions of $C_3A$ and $C_2A$ produce tricalcium

Received January 8, 2013; accepted March 26, 2013
*Corresponding author. E-mail: mafalda.guedes@estsetubal.ips.pt

disilicate hydrate (usually referred as C–S–H), responsible for most of the significant behavior and strength of the hardened cement and calcium hydroxide (CH).

Presence of the aggregate phase distributed throughout the cement paste imparts strength and dimensional stability to the material and decreases its cost. The main properties of the aggregates influencing concrete behavior are its density, shape, and size; pore structure, stability, and strength; as well as any surface characteristics affecting the bond to the paste (Domone, 1998). Concrete is thus commonly understood as a three-phase composite material including the hardened cement paste, the aggregate skeleton, and the interfacial transition zone (ITZ). The ITZ is the weakest phase because of its poorer cement particle packing and substantially higher porosity. Thus, cracking generally initiates within it (Domone, 1998; Poon et al., 2004; Scrivener et al., 2004). Details of the ITZ are expected to vary depending on cement content, water-to-cement ratio (w/c), aggregate composition and size distribution, curing conditions, and the presence of supplementary cementing components (fly ash, silica fumes, superplasticizers). ITZ characteristics vary from concrete to concrete, requiring dedicated investigation in a given case (Diamond, 2001). As a consequence, the internal structure of hydrated cement pastes and concretes is still poorly understood. In more recent years, studies have been reported regarding the use of crushed bricks, ceramic sanitary ware, and mixed ceramics waste as RCA (e.g., Cachim, 2009; Gomes & de Brito, 2009; Debieb & Kenai, 2008; Medina et al., 2012). However, most research focus on the comparison of physical and mechanical properties of recycled and conventional concrete, and their microstructural characterization is primarily limited to concretes prepared with common aggregates.

In this context, the current work renders a comparison between concrete containing natural aggregates and concrete reinforced with construction waste, focusing on the microstructural features of the ITZ.

## Materials and Methods

The studied concretes were prepared by mixing fine recycled aggregates (FRA) with natural aggregates, type I Portland cement, and water (Table 1). FRA were used to replace fine natural aggregates (FNA, sand) in extents of 10, 50, and 100 vol%, rendering in every case a total of 75.1 ± 1.0 wt% aggregates. Reference concrete (RC) with 0% substitution was also produced. The w/c ratio in the mixtures was kept at 0.55 ± 0.01.

The used recycled aggregates were obtained from a standard concrete (Table 2), processed and crushed under laboratory conditions (Evangelista & de Brito, 2007). Obtained aggregates were separated by mechanical sieving and only the size fraction below 4 mm was used, so that the particle size range of both FNA and FRA in the recycled concrete would be similar.

FNA and FRA were characterized by density and water absorption measurements following procedure described elsewhere (Evangelista & de Brito, 2007), and X-ray diffraction (XRD) (PW 3020, Philips, Eindhoven, The Netherlands). The produced concretes were cast in cylindrical wood molds with ∅100 × 200 mm, and kept at 20°C and 50% relative humidity. Hydration was stopped at the ages of 9, 24, and 96 h and 28 days; the collected samples were immediately immersed in ethanol 96 vol% in order to stop hydration reactions (Diamond, 2001), and kept in a desiccator, under vacuum. These samples were vacuum embedded with low viscosity epoxy resin followed by mechanical grinding and polishing with progressively fine abrasives down to 1 $\mu$m, according to the protocol described by Kjellsen et al. (2003). Field emission gun scanning electron microscopy (FEG-SEM) (JSM-7001F, JEOL, Tokyo, Japan) coupled with energy dispersive spectroscopy (EDS) microanalysis (Inca PentaFETx3, Oxford Instruments, Abingdon, Oxfordshire, UK) was used to study the new mixtures. Focus was placed on the ITZ between the cement matrix and aggregate, both on polished cross-sections and fracture surfaces. The profile for the ITZ was obtained from approximately 0–50 $\mu$m from the aggregate surface (Hussin & Poole, 2011). Attained materials were also characterized by XRD and hardness measurements (Officine Galileo, Campi Bisenzio, Florence, Italy). Mortars with the same base composition not containing coarse aggregates were also cast and subjected to 28-day wet curing, and test specimens were collected for mercury intrusion porosimetry (MIP) (Autopore IV 9600, Micromeritics, Norcross, GA, USA).

ImageJ (National Institutes of Health, Bethesda, MD, USA) was used to derive semiquantitative information con-

**Table 1.** Composition of the Produced Concretes.*

| Component | Sample Designation | | | |
|---|---|---|---|---|
| | RC | 10FRA | 50FRA | 100FRA |
| Replacement extent (vol%) | 0 | 10 | 50 | 100 |
| FRA (wt%) | 0.0 | 2.5 | 12.8 | 26.4 |
| CEM I 42.5R cement (wt%) | 15.6 | 15.7 | 16.2 | 16.7 |
| FNA (sand) (wt%) | 31.5 | 28.5 | 16.2 | 0.0 |
| CNA (gravel) (wt%) | 44.7 | 44.9 | 45.9 | 47.5 |
| Water (wt%) | 8.3 | 8.4 | 8.9 | 9.4 |
| w/c | 0.53 | 0.54 | 0.55 | 0.56 |

*RC, reference concrete; FRA, fine recycled aggregates; CNA, coarse natural aggregate; w/c, water-to-cement weight ratio.

**Table 2.** Composition of Original Concrete.

| Component | wt% |
|---|---|
| CEM II 42.5R cement | 7.9 |
| Sand | 23.1 |
| Fly ash | 4.8 |
| Coarse aggregate | 58.8 |
| Plasticizer | 0.1 |
| Water | 5.3 |

**Table 3.** Properties of the Aggregates in Study.*

| | FNA | FRA |
|---|---|---|
| Main components | $SiO_2$, $KAlSi_3O_8$ | $SiO_2$, $CaCO_3$ |
| Surface dry specific density ($g/cm^3$) | 2.56 | 2.19 |
| Water absorption (%) | 0.8 | 13.8 |
| $d_{10}$ (mm) | 0.25 | 0.13 |
| $d_{50}$ (mm) | 0.49 | 0.85 |
| $d_{90}$ (mm) | 1.40 | 3.55 |
| Calculated size span $(d_{90}–d_{10})/d_{50}$ | 2.3 | 4.0 |

*FNA, fine natural aggregates; FRA, fine recycled aggregates.

cerning porosity fraction and residual unhydrated cement fraction from backscattered electron images (BEI) of the ITZ. For this purpose, BEI were obtained at a magnification of 400× (Scrivener, 2004; Hussin & Poole, 2011) with 1,280 × 1,024 pixels resolution. All the images were first transformed into binary format and were then segmented to gray level binary segmentation to highlight the different features selected for analysis. Pixels corresponding to each of those components are separated by thresholding based on gray level: residual unhydrated cement is separated at the bright end of the gray scale [incorporation of water during hydration leads to hydrates with lower average atomic number than the anhydrous material (Scrivener, 2004)], whereas pores (filled with epoxy resin) are segmented at the dark end of the gray scale. The respective calculated area fraction was assumed to provide an adequate estimate of the vol% of the component (Diamond, 2001).

## Results

### Characterization of the Aggregates

The main properties of the natural and recycled aggregates in use are displayed in Table 3. Water absorption is significantly lower in FNA than in FRA, whereas its saturated density is somewhat higher. The used FRA presents higher median particle size than FNA (Fig. 1), together with a considerably broader particle size span. Regarding particle morphology, both FNA and FRA have an irregular surface and angular shape (Figs. 1, 2). FRA (Fig. 2) is a mixture of original FNA and bonded hydrated cement paste, as well as other unhydrated components. The aggregate/hydrated cement interface is well defined (Fig. 2b) and unhydrated fly ashes from the original cement are clearly visible as cenospheres. Capillary pores in the pore system are also visible.

### Characterization of Concretes Prepared with Natural Aggregates

The natural aggregate/cement interfacial zone exhibits typical microstructural features of the ITZ of a normal strength concrete. After 28 days, a large amount of well-crystallized C–S-H and poorly crystalline C–S-H fibers are present at the interface, together with large hexagonal crystals of CH (Fig. 3). In less mature concretes, C–S–H gel is discontinuous and less dense and CH crystals are scarcer than after 28 days. Grains of unreacted clinker components were also identified; some of the original components can be identified given their specific morphological features: this is the case of $C_2S$, which displays a typical cross-hatched appearance when partially hydrated (Diamond, 2004). Minor hydration products such as ettringite crystals (or monosulfate) are barely visible as isolated deposits, even at the earlier hydration times.

Figure 4 shows that in concretes prepared with natural aggregates the innermost part of the cement grains remains in a nonhydrated condition: the relative proportion of unhydrated cores (Fig. 5) is bigger for younger concretes, but is still present after 28 days (∼5%). Mostly, these cement remnants are surrounded with hydration product shells of varying thickness. These elements are separated from each other by a groundmass of finer hydrated components (gel) of heterogeneous appearance, intermingled with pore spaces (occupied in this case by hardened epoxy resin and thus

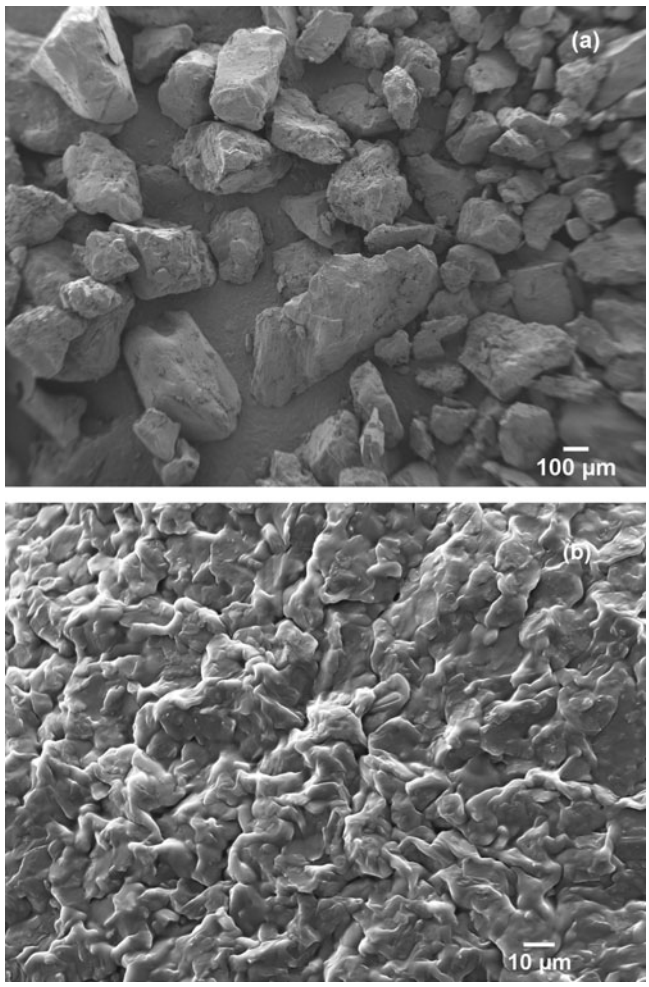


**Figure 1.** Natural sand used in preparation of the concretes in this study: (**a**) low-magnification image; (**b**) secondary electron image of the particles' surface.

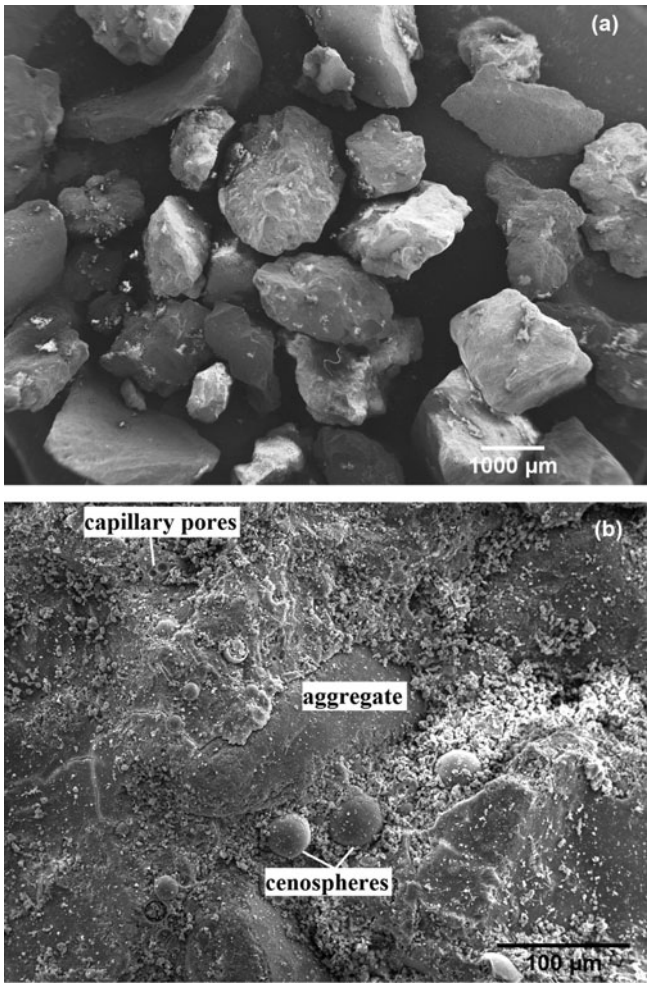


**Figure 2.** Secondary electron image of recycled aggregates: (**a**) low-magnification image; (**b**) surface of particles showing interface between original concrete and natural sand.

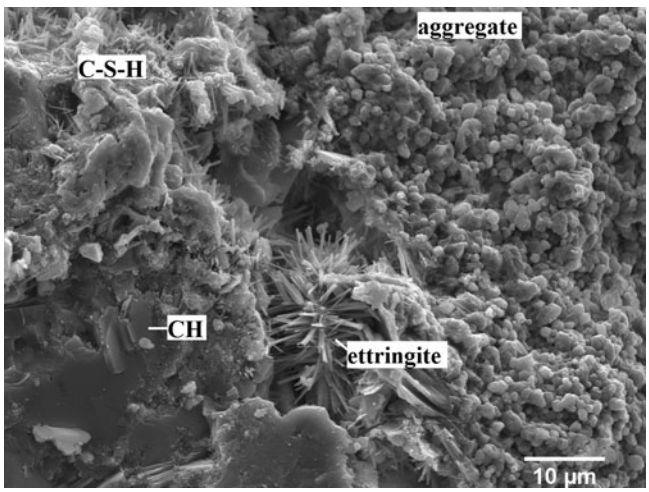


**Figure 3.** Interfacial transition zone in reference concrete (28 days).

segmented at the darker end of the grayscale). A significant content of pore space is visible for every hydration time, particularly at the ITZ. Image analysis results rendered 18.2 ± 1.9% porosity at the ITZ of RC. The mercury intrusion porosity of the material is approximately 10.26%, in good agreement with typical values reported in the literature (Diamond, 2004), and suggesting that porosity at the ITZ is noticeably higher than that of the bulk cement hydration products. Independently of the hydration time, fracture takes place preferably along the surface between paste and aggregate, attesting to the relatively loose nature of the interface in natural aggregate concrete.

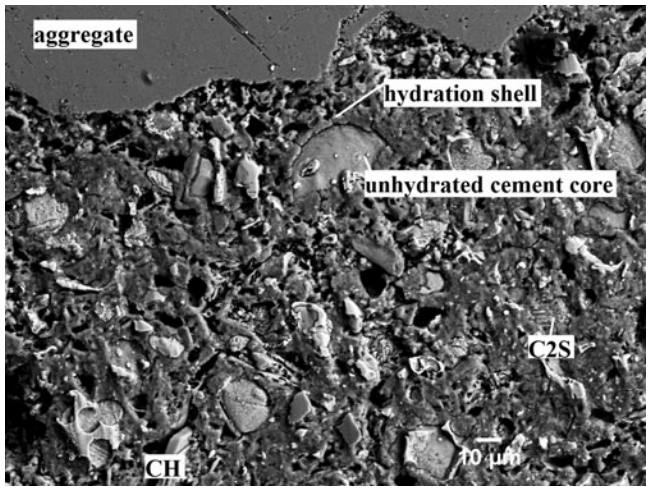


**Figure 4.** Low-magnification backscattered electron images of the interfacial transition zone in reference concrete (28 days).

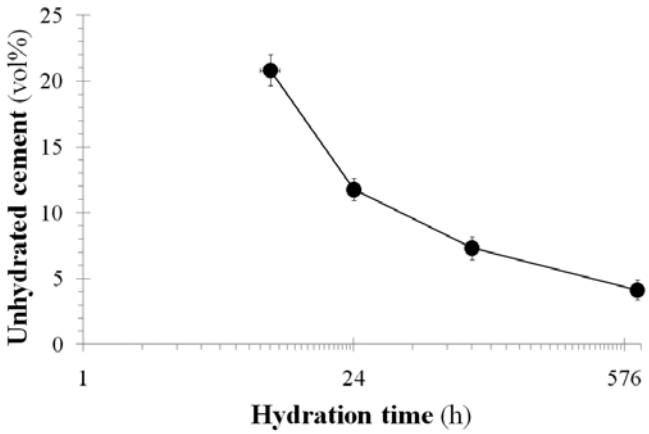


**Figure 5.** Unhydrated cement percentage at the interfacial transition zone for reference concrete.

## Characterization of Concretes Prepared with Recycled Aggregates

Microscopy studies of concrete mixtures with different substitution extent illustrate the effect of the incorporation of recycled aggregates on the formation and morphology of different concrete hydration products. As the chemical nature of the cement paste and recycled aggregates is the same, the identification of FRA (especially at the more mature ages) was made possible by their content in unhydrated fly ash, present as easily recognizable cenospheres. This allowed straightforward recognition between mature and fresh concrete (Fig. 6).

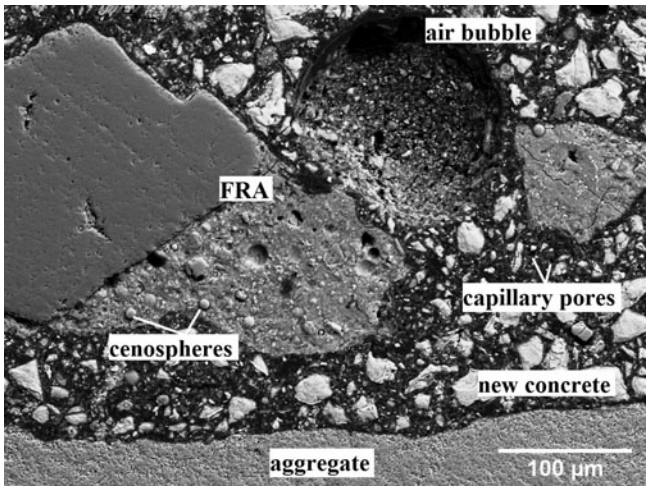


**Figure 6.** Low-magnification backscattered electron images of 100FRA concrete after 9 h hydration. FRA, fine recycled aggregates.

The overall structure of concrete containing FRAs in substitution of natural fine aggregates (sand) is consistent with that observed in the reference natural concrete (Fig. 4) at all ages. In addition, calculation based on EDS results rendered a lime to silica ratio (C/S) of $1.46 \pm 0.15$, consistent with the typical 1.2–2.3 range (Domone, 1998).

The main hydration products, C–S–H (gel and fibers) and CH, are distinctively deposited around the aggregates at such early times as 9 h (Fig. 7a). As the hydration time increases up to 28 days, all specimens are substantially densified (Fig. 7b), regardless of the substitution extent, without significant morphological change in the hydrates when compared with RC.

There are, however, representative microstructural features differing from the RC, and which may contribute to variation of mechanical properties. Large amounts of ettringite can be easily recognized, even at higher hydration times, and plate-like C–H hydrates are also much more abundant (Fig. 8). In addition, products from reaction between active silica in the fly ash of residual cementitious materials and fresh cement hydration products partially cover the pore structure of recycled aggregates (Fig. 9).

With regard to porosity at the ITZ, results from image analysis show that when recycled aggregates are added as a concrete raw material the associated variation in the concrete porosity volume fraction depends on the substitution extent. The introduction of 10 vol% recycled aggregates results in porosity decrease (Fig. 10), for every aging time. The porosity decrease reaches a reduction of approximately 12, 8, 15, and 12%, for 9, 24, 96 h, and 28-day hydration time, respectively. For higher aggregate replacement, porosity increases regardless of the hydration time; the maximum porosity increase always occurs for 100% replacement. This trend accompanies the overall porosity variation for the bulk concretes measured by MIP (Fig. 11, Table 4), with the exception of the behavior for 10 vol% substitution. The difference in porosity value associated with the ITZ and with the bulk cement phase after 28 days is around 8% for

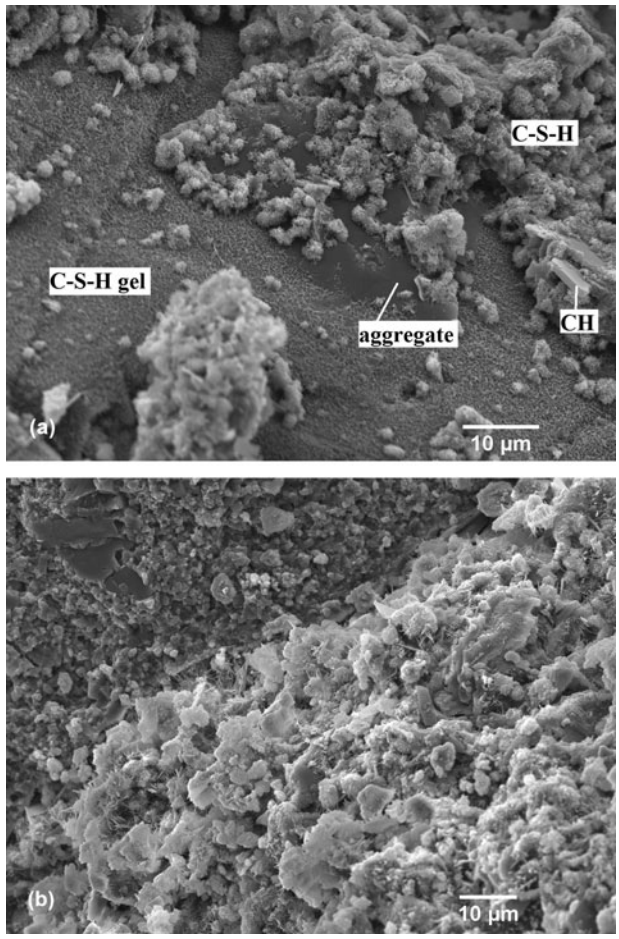


**Figure 7.** Secondary electron image of fracture surface of 10FRA concrete after hydration time of (**a**) 9 h and (**b**) 96 h. FRA, fine recycled aggregates.

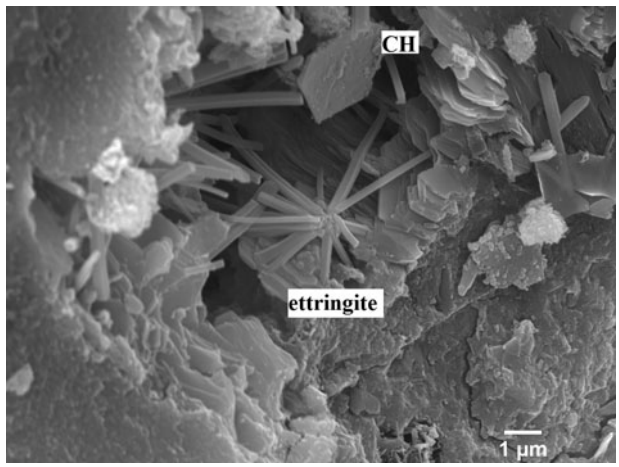


**Figure 8.** Interfacial transition zone in 100FRA concrete: secondary electron image showing ettringite and CH concealed in a pore after 96-h hydration time. FRA, fine recycled aggregates.

every substitution extent except 10 vol%, where the porosity difference is down to 4.7%. The pore size distribution in mortars where FNA was replaced by FRA is shown in Figure 11 and compared with that of the reference mortar

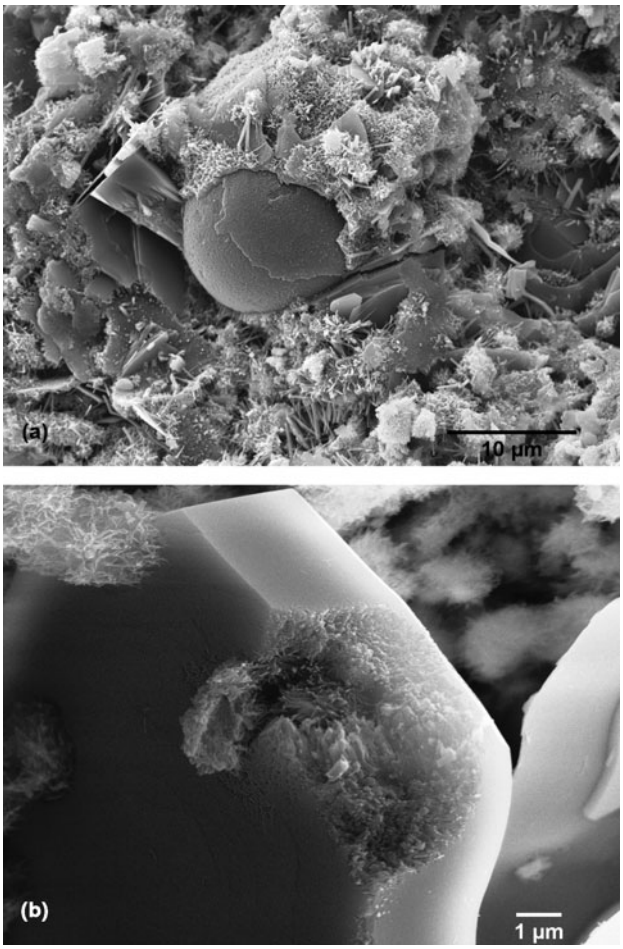


**Figure 9.** Secondary electron image of fracture surface showing secondary reaction features in substituted concrete: (**a**) reaction products (10FRA, 96 h); (**b**) CH attack (100FRA, 9 h). FRA, fine recycled aggregates.

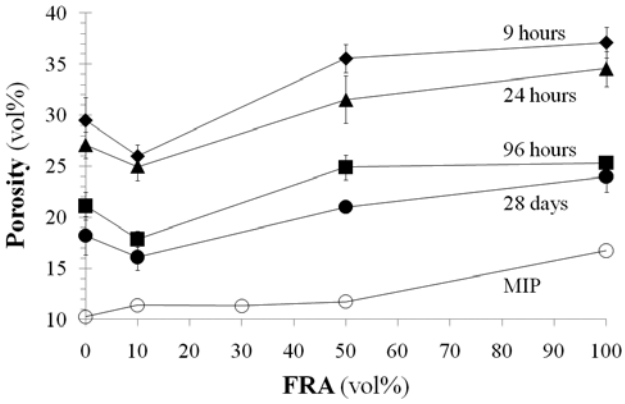


**Figure 10.** Porosity contents at the interfacial transition zone for natural and recycled aggregates [mercury intrusion porosimetry (MIP) curve refers to 28 days' hydration]. FRA, fine recycled aggregates.

without substitution after 28 days' hydration. The shape of the curves obtained for concrete with aggregate substitution is comparable to that of natural aggregate concrete. As expected (Domone, 1998), there is a continuous distribution of pore sizes, ranging from 0.006 to 350 $\mu$m in the studied mortars, with two maxima at both ends. Pores between C–S–H gel particles (gel pores), with a typical diameter between 0.0005 and 0.005 $\mu$m (Domone, 1998), are outside the MIP measuring range (Rübner & Hoffmann, 2006). Capillary pores, ranging between approximately 0.05 and 0.5 $\mu$m (Domone, 1998), correspond to the first observed maximum. Larger pores, at the microscopic end of the distribution, correspond to entrapped air bubbles, which are normally present in concrete as the result of incomplete compaction (Domone, 1998). At the microscopic range, the pore fraction decreases with increasing substitution extent, accompanied by a generalized shift of the capillary pores toward higher pore radii, and by an overall increase in total pore volume. These differences are less pronounced for 10FRA samples, whose distribution closely resembles the one for the RC.

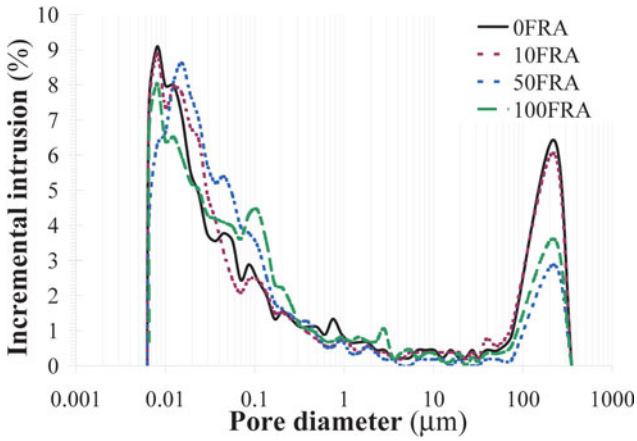


**Figure 11.** Incremental pore volume distribution curve (mercury intrusion porosimetry) for concrete with different substitution extents (28 days). FRA, fine recycled aggregates.

The presence of FRA also appears to significantly affect the cement hydration extent. The estimated unhydrated cement contents in the ITZ for the less mature and for 28-day hydration concrete is illustrated in Figure 12. As expected, the hydration level increases with hydration time, regardless of the substitution extent. In addition, the higher the replacement level, the higher the hydration degree.

In substituted concretes, fracture preferably takes place throughout the paste (Fig. 13) rather than through the paste/aggregate contact surface.

**Table 4.** Pore Size Distribution and Overall Porosity Obtained by Mercury Intrusion Porosimetry for Concretes with 28-Day Hydration Time.

| | 0FRA[a] | 10FRA | 50FRA | 100FRA |
|---|---|---|---|---|
| $d_{10}$ ($\mu$m) | 15.0 | 10.3 | 0.4 | 2.0 |
| $d_{50}$ ($\mu$m) | 0.030 | 0.0275 | 0.032 | 0.040 |
| $d_{90}$ ($\mu$m) | 0.009 | 0.009 | 0.010 | 0.009 |
| Porosity (%) | 10.26 | 11.39 | 11.76 | 16.75 |

[a]FRA, fine recycled aggregates.

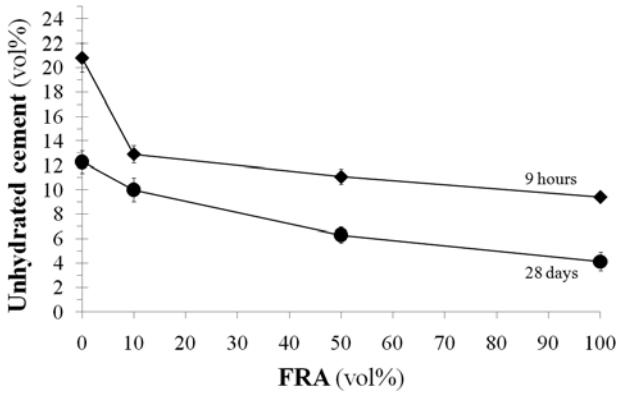


**Figure 12.** Unhydrated cement content at the interfacial transition zone for natural and recycled aggregate concrete after hydration time of 9 h and 28 days. FRA, fine recycled aggregates.

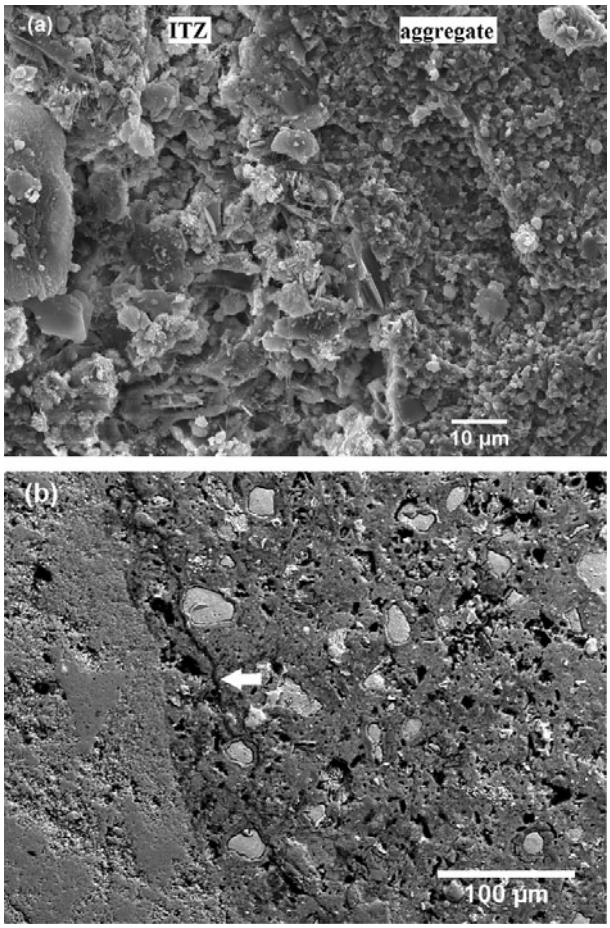


**Figure 13.** Secondary electron image (SEI) showing typical fracture propagation at the paste/aggregate interface in 100FRA concrete (28 days): (**a**) SEI of the interfacial bonding; (b) backscattered electron images of the strong interface, with fracture taking place throughout the paste (arrow). ITZ, interfacial transition zone; FRA, fine recycled aggregates

A hardness value of 83.0 ± 10.1 HR15T was obtained for the recycled aggregates in this study. Attained hardness values for a 28-day concrete were preferably obtained away from the aggregates, in the cement paste (Fig. 14). In the absence of substitution, the paste has a hardness value of 56.1 ± 2.6 HR15T. This value increases to 73.6 ± 3.9 HR15T for 10% substitution. Further substitution resulted in a decrease down to around 30 HR15T.

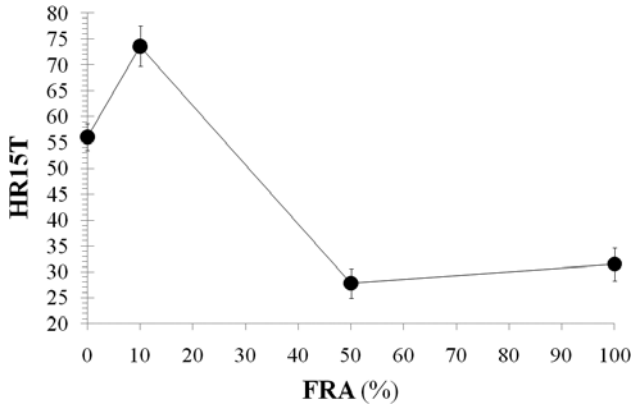


**Figure 14.** Hardness results for concrete after 28 days' hydration as a function of the substitution extent.

## Discussion

The use of aggregate with variable properties renders concretes with different features, mainly resulting from the different interfacial cement/aggregate microstructures established. Results obtained in this work with aggregate derived from CDW are discussed.

The properties of the recycled aggregate derived from crushed concrete are significantly different from those of natural aggregate. Recycled aggregates are heterogeneous because they combine natural aggregate and cement paste residue (Fig. 2b). The porous nature of the adhered old cement paste is expected to be responsible for the higher porosity (and lower density) of the recycled aggregates, thus resulting in a substantial difference in the determined water absorption capacity, which was found to be 13.8% for FRA (Table 3). This value is much higher than that of FNA, for which absorption was only about 0.8%.

The substitution of FNA by FRA does not change the composition or the morphology of the typical products resulting from the cement hydration process. However, different microstructural features arise: CH and ettringite are apparently more abundant and the concrete pore structure is significantly altered. The pore system in cement-based materials consists of four features (Kumar & Bhattacharjee, 2003): (i) micropores in the 0.5 to 10 nm range (gel pores), (ii) mesopores in the 5 to 5,000 nm range (capillary pores), (iii) macropores formed on compaction, and (iv) shrinkage cracks. The pore system in the FRA concrete mortar is markedly different from that in FNA mortar prepared independently under the same conditions: the difference is due to the pores present at the cement/aggregate ITZ (Kumar & Bhattacharjee, 2003). The difference between porosity results obtained by MIP and by image analysis was used to obtain a semiquantitative evaluation of bulk concrete apparent porosity versus porosity at the ITZ. It should be men-

tioned that gel pores remain nonintruded and are not quantified in MIP (Kumar & Bhattacharjee, 2003); in addition, pores smaller than a single pixel cannot be computed in the area fraction of pores, and thus capillary pores cannot be separated from gel pores by the gray level thresholding in image analysis (Diamond, 2001). However, gel pores do not adversely affect the mechanical properties of concrete (Kumar & Bhattacharjee, 2003) and were thus not included in the following analysis. The inclusion of recycled aggregate causes a refinement of the pore system, increasing the volume of capillary pores and decreasing the volume of macropores (Fig. 11). Overall porosity of the concretes increases with substitution extent (Fig. 10, MIP), presumably accompanied by an increased amount of absorbed water (Debieb & Kenai, 2008). However, porosity at the ITZ determined by image analysis (Fig. 10) does not follow the same trend, presenting a clear porosity decrease for a substitution extent of 10 vol% (and increasing for higher replacement values). In fresh natural concrete, the water film formed around the aggregates is gradually replaced by the growing amount of hydration products. In concrete containing RCA, active silica in residual cementitious materials reacts with water and fresh CH hydration products (Fig. 9), contributing with additional C–S–H (Domone, 1998; Poon et al., 2004). The presence of these secondary hydration reaction products is important in modifying the porosity at the ITZ (Scrivener et al., 2004), as they gradually fill the region, partially covering the recycled aggregates' pore structure and creating additional interfacial bonding. In good agreement, FEG-SEM observations generally revealed that the FNA/cement interface is relatively loose, as fracture takes place preferably throughout the contact surface, whereas in substituted concretes fracture preferably takes place throughout the paste (Fig. 13b). It is suggested that in the case of the introduction of 10FRA the amount of secondary hydrates produced was enough to compensate the introduced porosity increase. These results are in good agreement with other studies reporting that the use of porous aggregates can result in denser ITZ, as hydration products tend to migrate into the pores (Bruegel et al., 2004).

The occurrence of secondary hydration reactions together with the higher availability of water in the cement paste are also suggested to contribute to the decrease in the amount of unhydrated cement in the ITZ for higher substitution extents (Fig. 12).

The higher overall porosity of RCA concretes possibly explains the better ability to detect ettringite (and CH) in RCA concretes: ettringite that is intimately intermingled with C–S–H and CH in the ground mass is difficult to resolve in BEI (Diamond, 2004; Scrivener et al., 2004) and was found only in very small quantities in the RC. The higher amount of pores in RCA concrete supplied additional locations for the formation of isolated ettringite acicular crystals (as well as CH platelets), which remained undisturbed during sample preparation (Fig. 8). Another possibility is that the ions required for ettringite formation—which are very mobile in cement paste, including in mature concretes (Scrivener et al., 2004)—were supplied by the old cement paste in the RCA, where the ratio of $C_3S$ to calcium sulfate was possibly more favorable.

Microstructure and pore structure govern the macroscopic properties of concrete. Hardness results can be used to evaluate the sensitivity of the mechanical response of the bulk material to microstructural features (Igarashi et al., 1996). The replacement of 10 vol% of natural aggregate (~56 HR15T) by CDW results in a hardness increase of 48% (Fig. 14), whereas higher substitution fractions resulted in sharp hardness decreases to around 30 HR15T. The hardness increase for low substitution extents is suggested to be related with the recycled aggregates' ability to reinforce the aggregate/paste interfacial bond across the ITZ. This results from water absorption into the aggregate, leading to densification of the ITZ and improved bonding (Poon et al., 2004). It is expected that the introduction of porous CDW resulted in a stronger bond, capable of compensating for the negative effect due to the use of a weaker aggregate. For higher amounts of FRA, this compensation is no longer effective, and the hardness values further decrease to values below that of concrete reinforced with FNA. In a previous work (Pereira et al., 2012), the authors found a comparable trend regarding the compressive strength of similar compositions of concrete containing CDW. A value of $39.5 \pm 0.7$ MPa was found for concrete without substitution, whereas the replacement of 10 vol% of natural aggregate by FRAs resulted in a compressive strength of $40 \pm 1.1$ MPa (an increase of ~1.3%). Higher substitution extents resulted in compressive strength decrease, down to a minimum value around 38 MPa. These results suggest that substitution of FNA by FRA up to a limiting extent can actually result in increased mechanical strength, in agreement with results by other authors (e.g., Poon et al., 2004; Gomes & de Brito, 2009; Juan et al., 2010; Yang et al., 2011).

## Conclusions

The replacement of natural aggregates by recycled crushed concrete introduced different ITZ microstructures in the produced concrete, although it did not change the composition or the morphology of the typical products resulting from the cement hydration process. After 9 h to 28-day hydration, the recycled interface showed variation in both the porosity and the amount of hydration phases. In general, for all hydration times, the fraction of unhydrated cement phases decreased, whereas CH, ettringite, and porosity increased with increasing replacement amount. An exception was found for 10 vol% substitution, which presented lower porosity at the ITZ than the RC, regardless of the hydration time. The ITZ microstructural development appears to be an important factor governing mechanical strength in the recycled concrete: even if porosity at the ITZ increases with the extent of aggregate replacement, the interfacial bond is apparently stronger when recycled aggregates are used, at least up to a limiting substitution extent value.

Methods of modifying the ITZ are critical in the development of structural concrete, and the reported results suggest the viability of using waste from the construction and demolition industries as fine aggregate in the production of concrete. This envisages an opportunity window for the development of increased strength of Portland cement concretes using low added value concrete waste as raw material.

## Acknowledgment

The authors are grateful to Fundação para a Ciência e Tecnologia (FCT) for financial support under project PEst-OE/CTM/UI0084/2011.

## References

Bruegel, K.V., Koenders, E.A.B., Guang, Y. & Lura, P. (2004). Modelling of transport phenomena at cement matrix-aggregate interfaces. *Interf Sci* **12**, 423–431.

Cachim, P.B. (2009). Mechanical properties of brick aggregate concrete. *Constr Build Mater* **23**, 1292–1297.

Debieb, F. & Kenai, S. (2008). The use of coarse and fine crushed bricks as aggregate in concrete. *Constr Build Mater* **22**, 886–893.

Diamond, S. (2001). Considerations in image analysis as applied to investigations of the ITZ in concrete. *Cem Concr Comp* **23**, 171–178.

Diamond, S. (2004). The microstructure of cement paste and concrete—A visual primer. *Cem Concr Comp* **26**, 919–933.

Domone, J.L. (1998). Concrete. In *Construction Materials: Their Nature and Behaviour*, Illston, J.M. (Ed.), pp. 89–195. London, UK: E & FN Spon.

Evangelista, L. & de Brito, J. (2007). Mechanical behaviour of concrete made with fine recycled concrete aggregates. *Cem Concr Comp* **29**, 397–401.

Gomes, M. & de Brito, J. (2009). Structural concrete with incorporation of coarse recycled concrete and ceramic aggregates: Durability performance. *Mater Struct* **42**, 663–675.

Hussin, A. & Poole, C. (2011). Petrography evidence of the interfacial transition zone (ITZ) in the normal strength concrete containing granitic and limestone aggregates. *Constr Build Mater* **25**, 2298–2303.

Igarashi, S., Bentur, A. & Mindess, S. (1996). Microhardness testing of cementitious materials. *Adv Cem Based Mater* **4**, 48–57.

Juan, A., Medina, C., Guerra, M.I., Llamas, B., Morán, J.M. & Tascón, A. (2010). Re-use of construction and demolition residues and industrial wastes for the elaboration or recycled eco-efficient concretes. *Spanish J Agric Res* **8**, 25–34.

Kjellsen, K.O., Monsøy, A., Isachsen, K. & Detviller, R.J. (2003). Preparation of flat-polished specimens for SEM-backscattered electron imaging and X-ray microanalysis—importance of epoxy impregnation. *Cem Concr Res* **33**, 611–616.

Kumar, R. & Bhattacharjee, B. (2003). Porosity, pore size distribution and in situ strength of concrete. *Cem Concr Res* **33**, 155–164.

Medina, C., Frías, M. & Sánchez de Rojas, M.I. (2012). Microstructure and properties of recycled concretes using ceramic sanitary ware industry waste as coarse aggregate. *Constr Build Mater* **31**, 112–118.

Pereira, P., Evangelista, L. & de Brito, J. (2012). The effect of superplasticisers on the workability and compressive strength of concrete made with fine recycled aggregates. *Constr Build Mater* **28**, 722–729.

Poon, C.S., Shui, Z.H. & Lam, L. (2004). Effect of microstructure of ITZ on compressive strength of concrete prepared with recycled aggregates. *Constr Build Mater* **18**, 461–468.

Rübner, K. & Hoffmann, D. (2006). Characterisation of mineral building materials by mercury-intrusion porosimetry. *Part Part Syst Charact* **23**, 20–28.

Scrivener, K.L. (2004). Backscattered electron imaging of cementitious microstructures: Understanding and quantification. *Cem Concr Comp* **26**, 935–945.

Scrivener, K.L., Crumbie, A.K. & Laugesen, P. (2004). The interfacial transition zone (ITZ) between cement paste and aggregate in concrete. *Interf Sci* **12**, 411–421.

Yang, J., Du, Q. & Bao, Y. (2011). Concrete with recycled concrete aggregate and crushed clay bricks. *Constr Build Mater* **25**, 1935–1945.